THEORETICAL INVESTIGATION OF EXTENDED DEFECTS IN GROUP-III NITRIDES

A.F. WRIGHT
Semiconductor Material and Device Sciences Department, Sandia National Laboratories, Albuquerque, NM 87185-1415, afwrigh@sandia.gov

ABSTRACT

We have investigated two types of extended defects commonly found in AlN, GaN and InN films using density-functional techniques. First, basal-plane stacking faults have been studied for all three compounds. Stacking-fault energies were found to be largest in AlN and smallest in GaN consistent with density-functional results for their wurtzite/zinc-blende energy differences. In addition, the 4H and 6H structures were found to have lower energies than zinc blende for all three compounds. Second, we have investigated the electronic structure and formation energy for an edge dislocation in AlN. The full-core dislocation structure was found to have a filled electronic level approximately 0.55 eV above the valence-band edge and an empty level 1.4 eV below the conduction-band edge. An open-core structure was found to have filled and empty electronic levels closer to the middle of the energy gap. Formation energies for these two geometries suggest that the full-core structure would be expected to form in *p*-type material whereas both are expected in *n*-type material.

INTRODUCTION

Studies using transmission electron microscopy (TEM) show that heteroepitaxial group-III nitride films contain large numbers of extended defects including grain boundaries, dislocations and stacking faults.[1-6] In general, defect densities are largest near the substrate/film interface, but decrease markedly within the first 0.5 μm of film growth. Stacking faults are most often observed near the interfacial region of heteroepitaxial films,[5, 7] but have also been seen in bulk GaN crystallites.[8] Furthermore, nominal zinc-blende films typically contain numerous stacking faults, particularly in the case of AlN and InN.[9] The region above the first 0.5 μm contains mostly threading dislocations with densities in the range from 10^8 to 10^{10} per cm^2 (several orders of magnitude larger than observed in high quality group-III phosphide and arsenide films). Despite their abundance, very little is known about the electrical or optical properties of these dislocations, or about the structures and energies of stacking faults in the group-III nitrides. In order to gain insight into these defects and their properties, we have performed density-functional calculations for stacking faults in AlN, GaN and InN, and for an edge dislocation in AlN.

STACKING FAULTS IN AlN, GaN AND InN

AlN, GaN and InN differ from most other III-V semiconductors in that their ground-state crystal structure is wurtzite. The wurtzite (2H) structure is characterized by the stacking sequence ...ABABABAB... along the [0001] direction perpendicular to the basal plane, whereas the zinc-blende (3C or sphalerite) structure typical of most other semiconductors has the stacking sequence ...ABCABCABC... perpendicular to the [111] direction. In this notation, each letter stands for an ordered pair of cation and anion layers (we refer to this ordered-pair as simply a layer) and a particular letter refers to the atoms being placed at one of the three possible positions within the basal or (111) plane. In this regard, the wurtzite structure is distinguished by a stacking sequence with repeat period two while the zinc-blende structure has repeat period three. A basal-plane stacking fault, whether in wurtzite or zinc blende, is simply a mistake in the normal stacking sequence. In the wurtzite structure, there are three types of faults denoted I_1, I_2 and E.[10] The I_1 (intrinsic) fault has stacking sequence ...AB<u>ABC</u>BCB... with a single unit of sphalerite stacking inserted into the wurtzite sequence. The I_2 (intrinsic) fault has stacking sequence

DISCLAIMER

...AB<u>ABCA</u>CA... containing two units of sphalerite stacking, and the E (extrinsic) fault has stacking sequence ...AB<u>ABCAB</u>AB... containing three sphalerite units.

A stacking-fault energy is defined as the energy difference between faulted and unfaulted structures. This difference is given in terms of either a unit area in the basal plane, or the area of a primitive unit cell in which case it is referred to as a reduced stacking-fault energy. In this study, stacking-fault energies were calculated using an approach employed previously by Cheng *et al.* [11] to study polymorphism in SiC. In this approach, the energy of a periodic sequence of N layers is cast in the form of a 1-dimensional Ising-type model

$$NE = NE_0 - \sum_{i,n} J_n \sigma_i \sigma_{i+n}. \quad (1)$$

Here, E_0 is a reference energy, J_n is an interaction energy between n^{th} neighbor layers, and the summations are over all N layers. The spin parameters, σ, are defined in terms of the ordering between adjacent layers. We have assigned AB, BC and CA pairs a value of +1 and BA, CB and AC pairs a value of -1 with assignments made moving from left to right through a stacking sequence. Interactions beyond the third-neighbor layers have been neglected yielding I_1, I_2 and E model energies given by the expressions $(-2J_1 + 4J_2 - 6J_3)$, $(-4J_1 + 4J_2 - 4J_3)$ and $(-6J_1 + 4J_2 - 6J_3)$, respectively.

The interaction energies were determined from density-functional calculations for the 2H, 3H, 4H and 6H polytypes. In these calculations, lattice constants within the basal plane and the separations between adjacent layers were fixed at the relaxed values found for wurtzite. As a result, we use the notation 3H for the unit cell with repeat period three instead of 3C which would denote the fully relaxed cubic structure. Model energies per layer for these polytypes are given by the expressions

$$E_{2H} = E_0 + J_1 - J_2 + J_3 \quad (2)$$

$$E_{3H} = E_0 - J_1 - J_2 - J_3 \quad (3)$$

$$E_{4H} = E_0 + J_2 \quad (4)$$

$$E_{6H} = E_0 - \frac{1}{3}J_1 + \frac{1}{3}J_2 + J_3. \quad (5)$$

The interaction energies were extracted from suitable combinations, substituting density-functional energies on the left-hand sides. General features of the density-functional calculations have been described previously.[12] Convergence of the polytype energies was achieved using a 120 Ryd energy cutoff for the plane-wave expansion in GaN and an 80 Ryd cutoff for the expansions in AlN and InN utilizing Troullier-Martins pseudopotentials[13]. Because of the need for high precision, we used large sets of Brillouin-zone sampling points corresponding to Monkhorst-Pack parameters[14] {7,7,12} for 2H, {7,7,8} for 3H, {7,7,6} for 4H, and {7,7,4} for 6H.

The calculated interaction energies are plotted in figure 1. A notable feature is that the interactions between nearest-neighbor layers in the nitride compounds are at least 15 times larger in magnitude than between second-neighbor layers. For comparison, we also show interactions calculated in the same manner for GaP and GaAs, as well as ones obtained previously by Cheng *et al.* for SiC.[11] As can be seen, nearest-neighbor interactions are also dominant in GaP and GaAs. For SiC, however, the second-neighbor interaction is about half the nearest-neighbor value. This particular relationship, together with the small third-neighbor interaction, results the prediction of a near degeneracy between the 3C, 4H and 6H structures in SiC. Given the dominance of the first-neighbor interactions in the nitrides, no such degeneracy is expected although this dominance does result in the polytype energies being ranked 2H, 4H, 6H and 3C according to increasing energy (see the discussion below). Another feature worth noting in figure 1 is that the nearest-neighbor

interactions are negative in the nitrides, whereas they are positive in the other Ga-V compounds. This difference follows from the different ground-state structures.

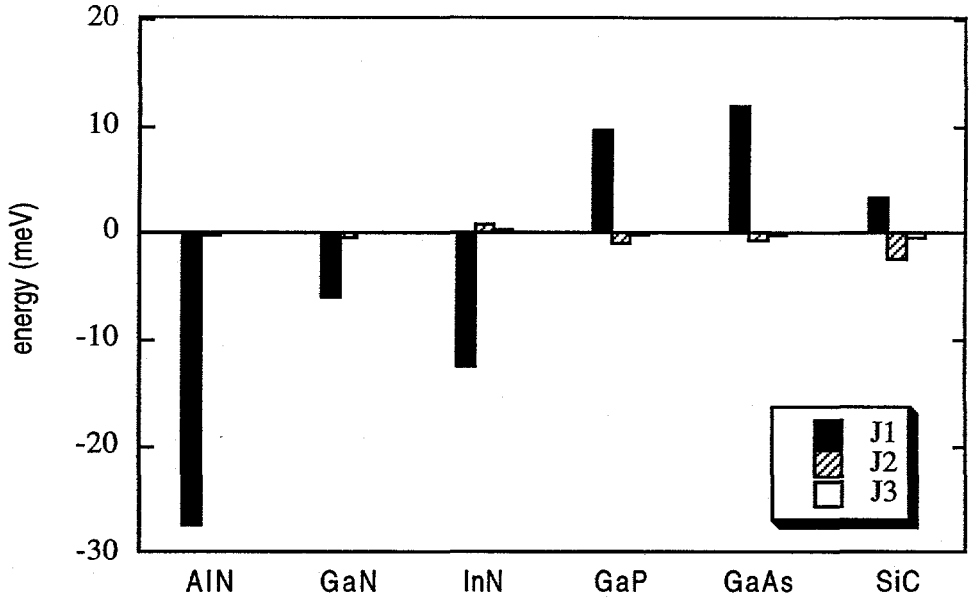

Figure 1. Reduced interaction energies in meV.

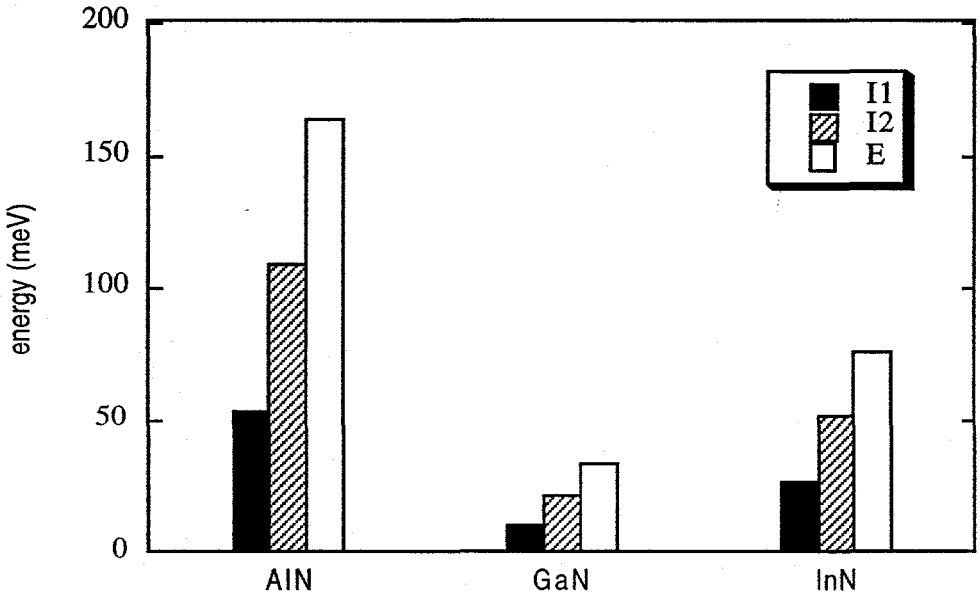

Figure 2. Wurtzite reduced stacking-fault energies in meV.

Our calculated stacking-fault energies are shown in figure 2. For all three compounds, the energies of the I_2 and E faults are two and three times larger, respectively, than the I_1 value. This relationship is expected from dominance of the nearest-neighbor interactions and the model expressions for the stacking-fault energies given above. In addition, we note that the relationship corresponds to the observation made earlier that the I_1, I_2 and E faults contain one, two and three sphalerite units, respectively. In comparing results among the three compounds, stacking-fault energies for AlN are seen to be largest while those for GaN are smallest. This ordering is consistent with the relaxed wurtzite/zinc-blende energy differences for these compounds. That is, the relaxed wurtzite/zinc-blende energy difference is largest for AlN and smallest for GaN. These results are shown explicitly in figure 3 together with relaxed energy differences for the 4H and 6H structures. As mentioned above, the fully relaxed 4H and 6H structures are predicted to have lower energies than the 3C structure, which previously had been assumed to have the lowest energy relative to wurtzite. In retrospect, this ordering is not surprising since the 4H and 6H structures can be thought of as having combinations of wurtzite and zinc-blende stacking. However, this simple correspondence would not necessarily hold if not for the dominance of nearest-neighbor interactions. In a related note, the dominance of the (positive-valued) nearest-neighbor interactions in GaP and GaAs suggests that the ordering of structures in these compounds should be 3C, 6H, 4H and 2H.

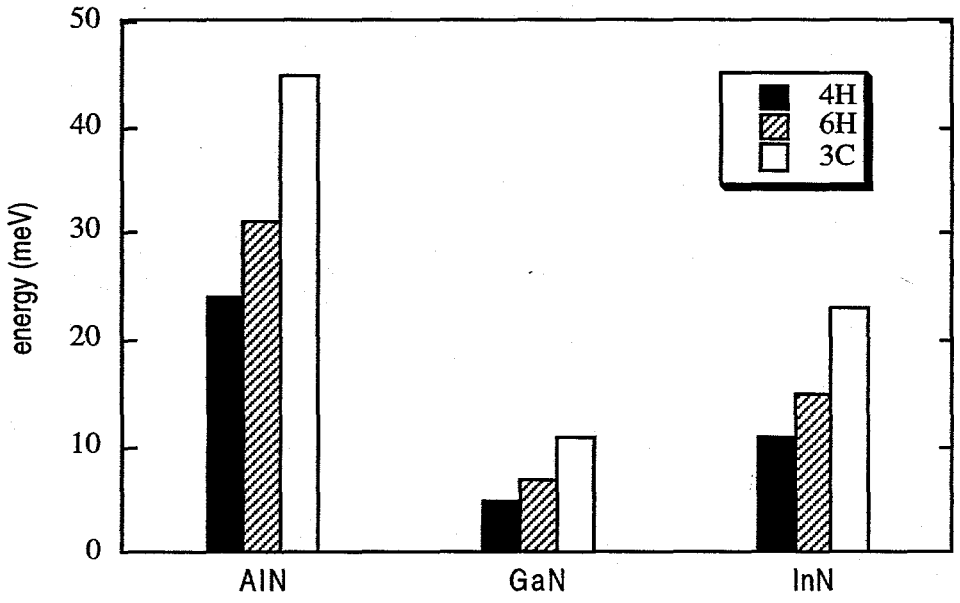

Figure 3. Polytype energies in meV per cation-anion pair.

To test the accuracy of our model results, we directly calculated the energy of the extrinsic fault in AlN using unit cells containing up to nine layers. The converged value (with respect to separation of repeated faults) was within 2% of the model value. We also examined the effect of relaxation perpendicular to the stacking direction for the case of the extrinsic fault in AlN (for which relaxations should be largest). Allowing full relaxation of the layer separations and cation-anion separations within each layer lowered the stacking-fault energy by less than 5% from the unrelaxed value.

To the best of our knowledge, there are no previous theoretical results for stacking fault energies in AlN, GaN or InN. There have been at least two attempts to estimate stacking-fault energies in the group-III nitrides based on experimental measurements. Suzuki *et al.* used high-

resolution TEM to observe lattice defects in AlN, GaN and InN.[15] From the spacing between Shockley partials in AlN and InN, they estimated reduced I_2 energies of 115 ± 36 meV for AlN and 27 ± 6 meV for InN. Our AlN value is within 5% of their estimate, but our InN value is twice theirs. Isolated Shockley partials were seen in GaN, but no pairs were seen from which spacings could be measured. This suggests that the stacking-fault energy is small in GaN which is qualitatively consistent with our results. The only other estimated value we are aware of from a study by Delavignette *et al.* which found the value 2 meV for I_2 in AlN [16] This value is much smaller than our result and the estimate of Suzuki *et al.*

Given our interaction energies, we can also estimate the energies of zinc-blende stacking faults. (These are rough estimates since the layer separations used in the polytype calculations were appropriate for wurtzite, not zinc blende.) Three types of faults are found in the zinc-blende structure denoted I (intrinsic), E (extrinsic), and T (twin). These faults have stacking sequences ...ABCBCABC..., ...ABCBABC..., and ...ABCABCBACBA... with corresponding model energies $(4J_1 + 4J_2 + 4J_3)$, $(4J_1 + 8J_2 + 8J_3)$, and $(2J_1 + 4J_2 + 6J_3)$. As is clear from the expressions, the estimated fault energies will all be negative (see figure 4). This is reasonable since the zinc-blende faults contain one or more units of the lower-energy wurtzite stacking. However, this result helps to explain the difficulty in growing zinc-blende films, particularly AlN and InN. The reduced energy of the wurtzite structure makes it energetically favorable to introduce stacking faults in zinc-blende films, thereby converting to the wurtzite structure. [9] This process should be especially favorable for AlN and InN which have larger wurtzite/zinc-blende energy differences than GaN and, correspondingly, larger magnitude stacking-fault energies.

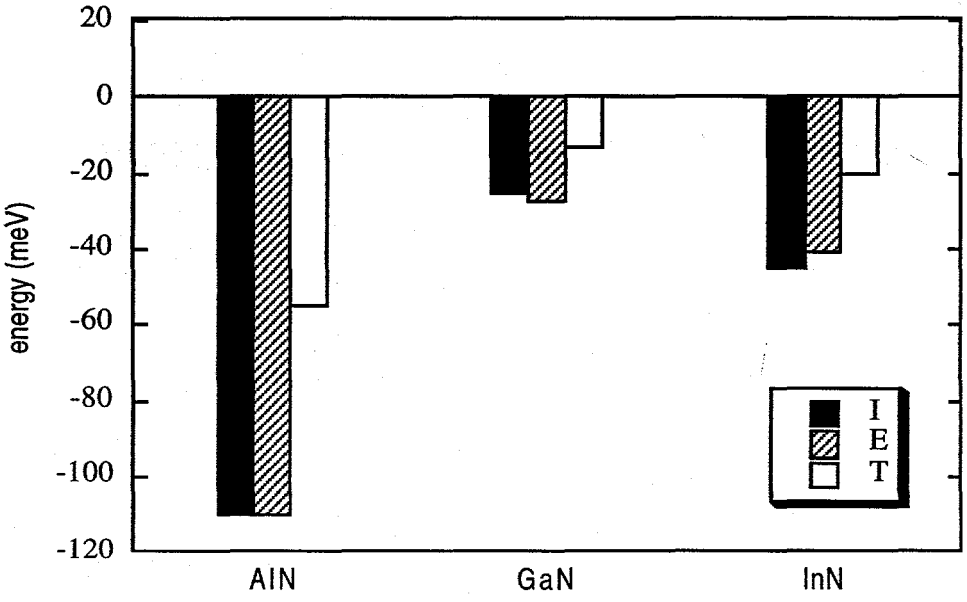

Figure 4. Zinc-blende reduced stacking-fault energies in meV.

EDGE DISLOCATIONS IN AlN

TEM studies on GaN films indicate that the observed threading dislocations are either edge type lying along the [0001] direction and having Burgers vector <11-20>/3, or mixed edge and screw type lying along the [0001] direction with Burgers vector <11-23>/3. We have performed density-functional calculations for the pure edge dislocation in AlN using the Vienna *ab initio*

simulation program (VASP).[17] A 112-atom unit cell containing two edge dislocations with opposite signs was used in these calculations and the Brillouin zone was sampled using Monkhorst-Pack parameters {2,2,2}. We considered both the full-core dislocation structure shown in figure 5 and also the open-core structure shown in figure 6. Total energies were calculated for these structures in various charge states and including full relaxation of the geometries. Their formation energies were then determined using the expression [18, 19]

$$E^f = E_{tot} - n_{AlN}\mu_{AlN} + qE_V + qE_F. \quad (6)$$

Here, E^f is the formation energy, E_{tot} is the total energy for the defect cell, n_{AlN} is the number of AlN units in the defect cell, μ_{AlN} is the calculated energy for bulk AlN, E_V is the energy of the valence-band maximum in bulk AlN (including a defect-cell-dependent shift[20]), q is the charge state, and E_F is the Fermi level defined to be zero at the bulk valence-band edge.

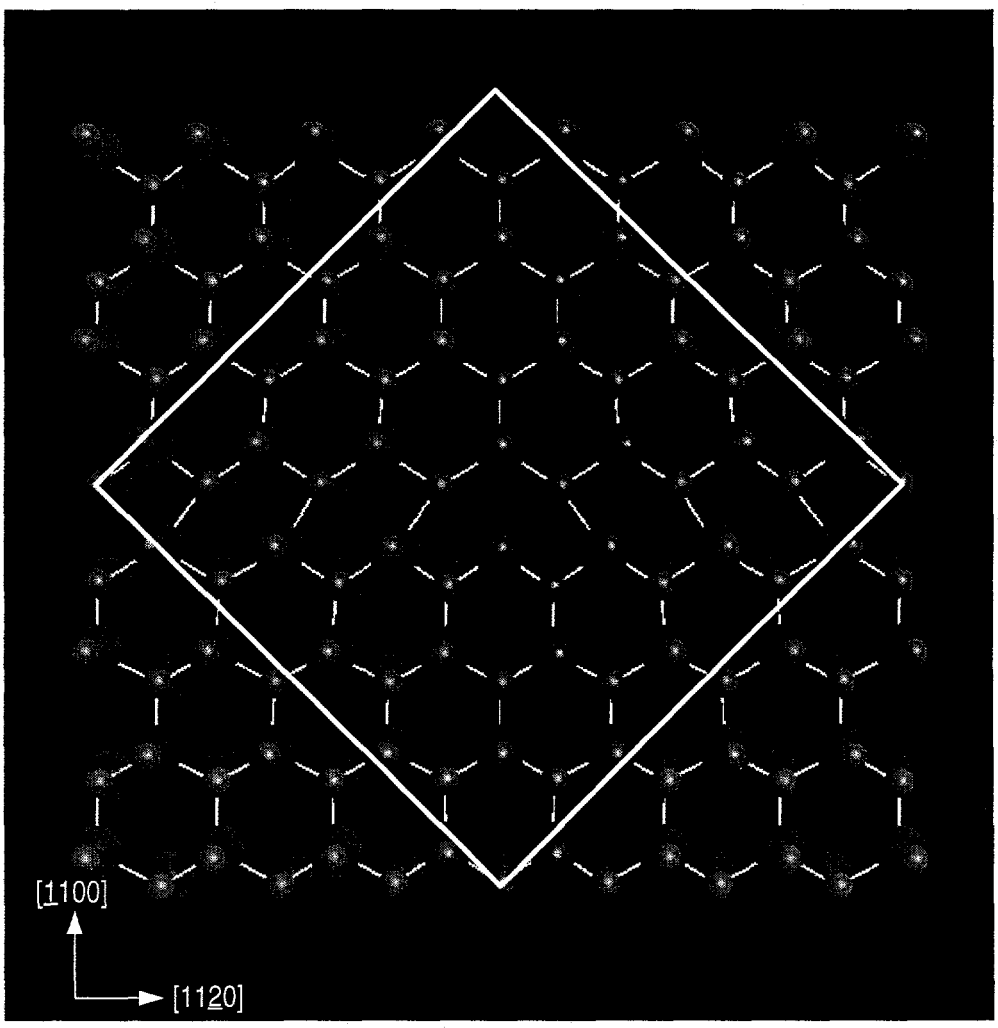

Figure 5. Full-core dislocation structure (the larger spheres denote Al atoms and the smaller spheres denote N atoms). The unit cell is outlined by white lines.

Plots of the formation energies vs. E_F for the two structures are shown in figure 7. The envelope corresponding to the lowest formation energy for each structure (depending on the charge state) is shown, and the slope of the plot at a particular point indicates the most stable charge state. The full-core structure, for example, is predicted to be in a +2 charge state for $E_F < 0.41$ eV, a +1 charge state for 0.41 eV $< E_F <$ 0.71 eV, a neutral charge state for 0.71 eV $< E_F <$ 4.90 eV, and a

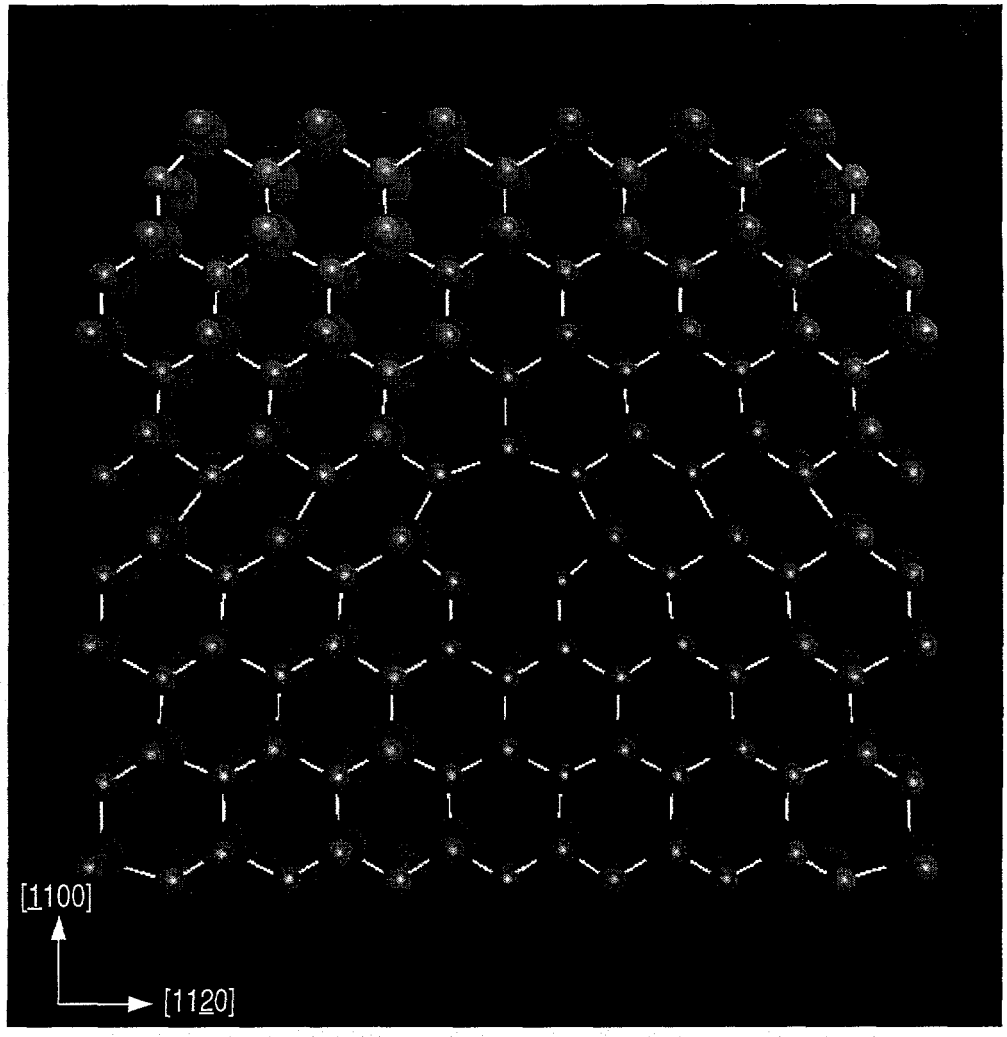

Figure 6. Open-core dislocation structure (the larger spheres denote Al atoms and the smaller spheres denote N atoms).

-2 charge state for $E_F > 4.90$ eV. Transitions between the different charge states occur where the plots change slope. The transition locations for the full-core structure indicate that it has a filled electronic level located approximately 0.55 eV above the valence-band edge and an unfilled electronic level 1.4 eV below the conduction-band edge. The filled state has *p*-character (similar to states at the valence-band maximum in bulk AlN) and is localized on the under-coordinated N atom at the edge of the dislocation. The unfilled state has *s*- and *p*-character (similar to states at the conduction-band minimum in bulk AlN) and is localized on the Al atom at the edge of the dislocation. This type of electronic structure is expected and is due to transfer of charge from the Al atom to the N atom which then can form a lone pair state having lower energy. The same type of rearrangement is not possible, however, in the open core structure because of the close proximity of the two sets of under-coordination atoms. As a result, filled and unfilled states in this structure are located deeper within the energy gap.

Test calculations on larger unit cells show that the formation energies themselves shift toward higher values with increased separation of the repeated dislocations. This is expected since strain fields due to the dislocations decay slowly with distance. Differences in the formation energies for the two structures, however, are converged to within about 0.5 eV for the 112-atom cell. As a result, the full-core structure is predicted to be stable for E_F below about 4.6 eV whereas the two structures are roughly equally favored above this value. Varying the Fermi level around this point (via doping) should therefore yield different dislocation structures in AlN.

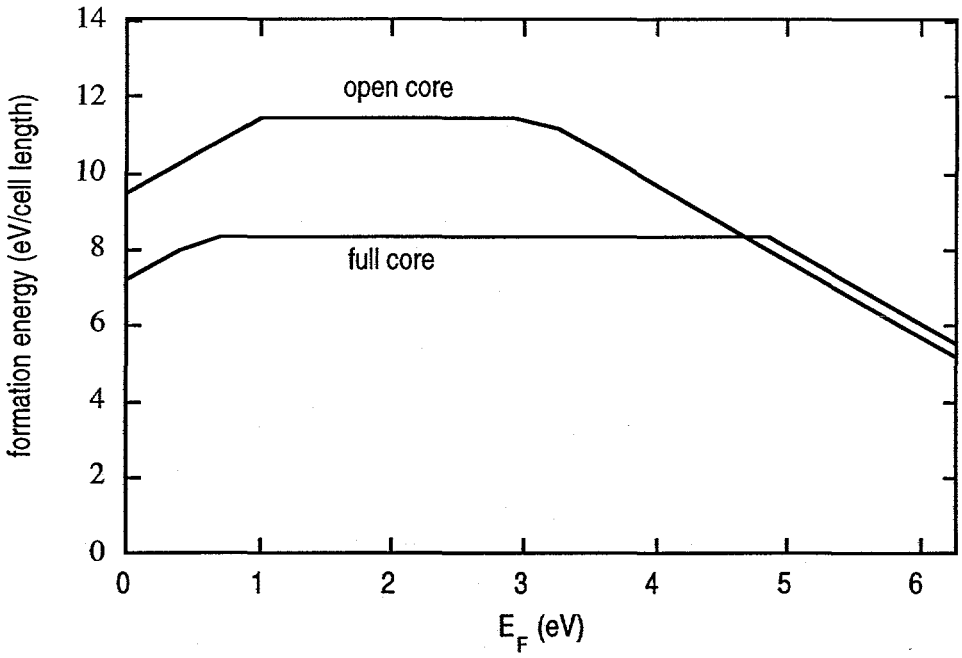

Figure 7. Formation energies for the full- and open-core structures.

CONCLUSIONS

We have calculated stacking-fault energies in wurtzite AlN, GaN and InN utilizing a 1-dimensional Ising-type model together with density-functional calculations for layer-layer interaction energies. The stacking-fault energies are found to be largest in AlN and smallest in GaN consistent with density-functional calculations for their wurtzite/zinc-blende energy differences. Corresponding estimates of the zinc-blende stacking-fault energies suggest that the zinc-blende structure is unstable with respect to faulting in all three compounds, but more so for AlN. This observation helps to explain the great difficulty in growing zinc-blende AlN films. Additionally, these calculations reveal that the 4H and 6H structures have lower energies than zinc blende for all three compounds.

Calculations have also been performed for an edge dislocation in AlN. Results for the full-core structure indicate that its neutral charge state consists of a filled level roughly 0.55 eV above the valence-band edge and an empty level 1.4 eV below the conduction-band edge. Results for an open-core structure show that it has a filled level 1.0 eV above the valence-band edge and an empty level roughly in the middle of the energy gap. Comparison of the formation energies for the two structures indicate that the full-core structure is favored in materials where the Fermi level is less than about 4.6 eV, while the two structures are equally favored for higher Fermi levels.

ACKNOWLEDGMENTS

This work was supported by the United States Department of Energy under Contract No. DE-AC04-94AL85000.

REFERENCES

1. Z. Sitar, M. J. Paisley, B. Yan, and R. F. Davis, Mat. Res. Soc. Symp. Proc. **162**, 537 (1990).

2. X. H. Wu, L. M. Brown, D. Kapolnek, S. Keller, B. Keller, S. P. DenBaars, and J. S. Speck, J. Appl. Phys. **80**, 3228 (1996).

3. Y. Xin, P. D. Brown, C. J. Humphreys, T. S. Cheng, and C. T. Foxon, Appl. Phys. Lett. **70**, 1308 (1997).

4. F. A. Ponce, D. Cherns, W. T. Young, and J. W. Steeds, Appl. Phys. Lett. **69**, 770 (1996).

5. Z. Liliental-Weber, H. Sohn, N. Newman, and J. Washburn, J. Vac. Sci. Technol. B **13**, 1578 (1995).

6. S. D. Lester, F. A. Ponce, M. G. Craford, and D. A. Steigerwald, Appl. Phys. Lett. **66**, 1249 (1995).

7. X. H. Wu, D. Kapolnek, E. J. Tarsa, B. Heying, S. Keller, K. B. P., U. K. Mishra, S. P. DenBaars, and J. S. Speck, Appl. Phys. Lett. **68**, 1371 (1996).

8. Z. Liliental-Weber, C. Kisielowski, S. Ruvimov, Y. Chen, J. Washburn, I. Grzegory, M. Bockowski, J. Jun, and S. Porowski, J. Elect. Mater. **25**, 1545 (1996).

9. S. Strite, M. E. Lin, and H. Morkoç, Thin Solid Films **231**, 197 (1993).

10. D. Hull and D. J. Bacon, *Introduction to Dislocations* (Pergamon Press, Oxford, 1984), p. 114.

11. C. Cheng, R. J. Needs, and V. Heine, Journal of Physics C: Solid State Physics **21**, 1049 (1988).

12. A. F. Wright and J. S. Nelson, Phys. Rev. B **51**, 7866 (1995).

13. N. Troullier and J. L. Martins, Phys. Rev. B **43**, 1993 (1991).

14. H. J. Monkhorst and J. D. Pack, Phys. Rev. B **13**, 5188 (1976).

15. K. Suzuki, M. Ichihara, and S. Takeuchi, Jpn. J. Appl. Phys. **33**, 1114 (1994).

16. P. Delavignette, H. B. Kirkpatrick, and S. Amelinckx, J. Appl. Phys. **33**, 1098 (1961).

17. G. Kresse and J. Hafner, Phys. Rev. B **47**, 558 (1993); ibid. Phys. Rev. B **49**, 14251 (1994); G. Kresse and J. Furthmuller, Compt. Mat. Sci. **6**, 15 (1996); ibid. Phys. Rev. B **54**, 11169 (1996).

18. D. B. Laks, C. G. Van De Walle, G. F. Neumark, P. E. Blochl, and S. T. Pantelides, Phys. Rev. B **45**, 10965 (1992).

19. J. Neugebauer and C. G. Van de Walle, Phys. Rev. B **50**, 8067 (1994).

20. A. Garcia and J. E. Northrup, Phys. Rev. Lett **74**, 1131 (1995).